Hierarchy of partially synchronous states in a ring of coupled identical oscillators

Mei Zhang [1], Yuhe Yang, [2] and Junzhong Yang [3,*]

[1] *Department of Physics, Beijing Normal University, Beijing 100875, People's Republic of China*
[2] *School of Mathematics, Peking University, Beijing 100871, People's Republic of China*
[3] *School of Science, Beijing University of Posts and Telecommunications, Beijing 100876, People's Republic of China*

(Received 20 March 2023; revised 17 July 2023; accepted 25 August 2023; published 7 September 2023)

In coupled identical oscillators, complete synchronization has been well formulated; however, partial synchronization still calls for a general theory. In this work, we study the partial synchronization in a ring of N locally coupled identical oscillators. We first establish the correspondence between partially synchronous states and conjugacy classes of subgroups of the dihedral group D_N. Then we present a systematic method to identify all partially synchronous dynamics on their synchronous manifolds by reducing a ring of oscillators to short chains with various boundary conditions. We find that partially synchronous states are organized into a hierarchical structure and, along a directed path in the structure, upstream partially synchronous states are less synchronous than downstream ones.

DOI: 10.1103/PhysRevE.108.034202

I. INTRODUCTION

Systems composed of a number of interacting entities are prevalent in various fields ranging from physics, chemistry, to biology, and society [1–3]. Examples include neuronal systems in human beings [4], and ions trapped in an optical lattice [5]. Synchronization, oscillation quenching, and pattern formation in these systems have been hotspots over the past several decades [6–8]. Coupled oscillators offer a platform to investigate the dynamics in these systems. The often-opted simplest model is a chain of locally coupled identical oscillators with a periodic boundary condition, or in other words a ring of identical oscillators.

Synchronization in coupled oscillators refers to the phenomenon in which dynamical properties, such as rhythms, phases, and state variables, of oscillators are made to be in unison due to the coupling between them. The complete synchronization among all identical oscillators has already been well documented [9–14]. Partial synchronization in coupled identical oscillators, defined as one type of synchrony where some oscillators are in complete synchronization with each other and others do not [15], has also been observed and is thought to be intermediate between the desynchronization and the complete synchronization [16–23]. However, to the best of our knowledge, a systematic theory on partial synchronization even in a ring of locally coupled identical oscillators is still not conclusive in that a general classification of the partially synchronous states, or an effective recipe to find out all the partially synchronous states, remains elusive. Previous works on the related subject of phase-shift synchrony in networks may shed light on the investigation of partial synchronization [24–32]. In the phase-shift synchrony, oscillators have identical periodic dynamics except for fixed phase shifts for any pair of oscillators [24]. Considering that the topology of a network strongly constrains the dynamical behaviors on it, these works use group theory to predict spatiotemporal patterns required by the spatial symmetry of the network. Among these, the H/K theorem behind phase-shift synchrony classifies the possible spatiotemporal symmetries of periodic states for symmetric systems [24,25]. For example, Hunter and collaborators focused on a four-ring reaction-diffusion network to verify the predictions by the H/K theorem [26]. However, different from phase-shift synchrony, partial synchronization does not require the same trajectory for oscillators. How to apply the group theory to partial synchronization in coupled oscillators is a challenging problem.

Pattern formation in spatial-temporal systems is a long-standing subject in nonlinear dynamics and other fields [33]. It is usually believed that pattern formation is due to the existence of unstable spatial modes. Depending on the instabilities of corresponding spatial modes, the patterns formed may be Turing patterns [34,35] or wave propagations [36]. However, partial synchronization may appear in spatial-temporal systems as a different type of pattern formation, which may come by out of constituent modules and does not involve unstable spatial modes.

In this work, we study the partial synchronization in a ring of N locally coupled identical oscillators. We first establish the correspondence between a partially synchronous state and a subgroup of the dihedral group D_N and categorize partially synchronous states according to conjugacy classes of subgroups of D_N. Then we present a systematic method to identify all partially synchronous states by reducing a ring of oscillators to short chains with different types of boundary conditions. We find that different partially synchronous states are organized into a hierarchical structure which makes it possible to compare the degrees of synchronization of different partially synchronous states.

*jzyang@bupt.edu.cn

II. MODEL AND STATE CLASSIFICATION

We consider a chain of N locally coupled identical oscillators with a periodic boundary condition, denoted as $(N)_\mathrm{p}$. The equations of motion are

$$\dot{\mathbf{x}}_i = \mathbf{F}(\mathbf{x}_i) + \epsilon[\mathbf{H}(\mathbf{x}_{i+1}) + \mathbf{H}(\mathbf{x}_{i-1}) - 2\mathbf{H}(\mathbf{x}_i)], \tag{1}$$

where $\mathbf{x}_i$ is the state vector of the ith oscillator $(i = 1, \cdots, N)$ and the periodic boundary condition implies that $\mathbf{x}_0 \equiv \mathbf{x}_N$ and $\mathbf{x}_{N+1} \equiv \mathbf{x}_1$. The function $\mathbf{F}$ describes the dynamics of a single oscillator while $\mathbf{H}$ the interaction between oscillators, and the parameter ϵ represents the coupling strength.

To begin, we claim that model (1) possesses the symmetry described by the dihedral group D_N of order $2N$. Mathematically, the group is represented as $D_N = \langle \sigma, \tau | \sigma^N = \tau^2 = e, \tau\sigma\tau = \sigma^{-1} \rangle$ with e the identity while σ and τ its two generators representing, respectively, the elementary rotation and reflection. For identical oscillators, model (1) is invariant under two types of fundamental operations, the rotation and the reflection. The rotation on model (1) is defined by the transformation: $\mathbf{x}_i \to \mathbf{x}_{i-k}$ with $k \in \{0, ..., N-1\}$, represented by the element σ^k in D_N. However, the reflection is represented by $\sigma^k\tau$ in D_N, which is the elementary reflection τ followed by k successive elementary rotations. The reflection axis of $\sigma^k\tau$ depends on the choice of the axis of τ and whether k and N are even or odd. The elementary rotation σ is fixed in a counter-clockwise direction. For odd N, if the axis of τ is the bisector through oscillator N, then the reflection $\sigma^k\tau$ simply refers to the transformation $\mathbf{x}_{\frac{k}{2}+i} \to \mathbf{x}_{\frac{k}{2}+N-i}$ for even k and $\mathbf{x}_{\frac{k+N}{2}+i} \to \mathbf{x}_{\frac{k+N}{2}+N-i}$ for odd k, and the reflection axis is the bisector through oscillator $\frac{k}{2}$ and $\frac{k+N}{2}$, respectively. In contrast, for even N, if the axis of τ is the bisector through the midpoint of the edges connecting oscillators 1 and N, then the reflection $\sigma^k\tau$ describes either $\mathbf{x}_{\lceil\frac{k}{2}\rceil+i+1} \to \mathbf{x}_{\lceil\frac{k}{2}\rceil+N-i}$ or $\mathbf{x}_{\lceil\frac{k}{2}\rceil+i} \to \mathbf{x}_{\lceil\frac{k}{2}\rceil+N-i}$ ($\lceil\cdot\rceil$ stands for the ceil of $\cdot$) depending on k even or odd, with the reflection axis being the bisector either crossing the midpoint of oscillators $\lceil\frac{k}{2}\rceil$ and $\lceil\frac{k}{2}\rceil + 1$ or passing through oscillator $\lceil\frac{k}{2}\rceil$, respectively. Two specific examples, $N = 3$ and $N = 4$, to demonstrate the rotation and reflection operations, are given in Fig. 7 in the Appendix.

Next we claim that partially synchronous states in model (1) are represented by subgroups of D_N. For any partially synchronous state in model (1), there exist at least two oscillators in the same state, such as oscillators i and j satisfying $\mathbf{x}_i(t) = \mathbf{x}_j(t)$. We further assume that no other oscillators in between are in synchronization with these two oscillators. According to model (1), the synchronization between oscillators i and j indicates $\mathbf{H}(\mathbf{x}_{i+1}) + \mathbf{H}(\mathbf{x}_{i-1}) = \mathbf{H}(\mathbf{x}_{j+1}) + \mathbf{H}(\mathbf{x}_{j-1})$. The equality gives rise to two possible situations: (I) $\mathbf{x}_{i+1}(t) = \mathbf{x}_{j+1}(t)$ and $\mathbf{x}_{i-1}(t) = \mathbf{x}_{j-1}(t)$; (II) $\mathbf{x}_{i+1}(t) = \mathbf{x}_{j-1}(t)$ and $\mathbf{x}_{i-1}(t) = \mathbf{x}_{j+1}(t)$. That is, any two oscillators in synchronization should be in the same environment. Situation I leads to a partially synchronous state which is invariant under the rotation σ^k with $k = \min\{|i-j|, N-|i-j|\}$. In contrast, situation II leads to a partially synchronous state with the reflection symmetry. The axis of reflection symmetry passes oscillator $\frac{i+j}{2}$ for even $i+j$ or lying between oscillators $\frac{i+j-1}{2}$ and $\frac{i+j+1}{2}$ for odd $i+j$. Therefore, all partially synchronous states in model (1) are invariant under at least one elementary operation, either the rotation or the reflection. If we suppose there is a set whose elements keep a partially synchronous state invariant, then it can be easily proven that the set must be a subgroup of D_N. So each partially synchronous state in model (1) is represented by at least one subgroup of D_N. In fact, there exist two trivial subgroups of D_N, the set consisting of only the identity and D_N itself, the former accounting for the desynchronous state while the latter the completely synchronous state. Based on the connection between the partially synchronous states in model (1) and subgroups of D_N, we can exclude the existence of partially synchronous states in model (1) if they are not invariant under the operations of any subgroup of D_N, for example the one in which two oscillators i and j are synchronized whereas all the others are not when $N > 3$.

Furthermore, we claim that partially synchronous states in model (1) are classified by the conjugacy classes of subgroups of D_N. Consider a ring of four identical oscillators. The partially synchronous state "ABBA" is represented by the subgroup $\langle\sigma\tau\rangle$ while "AABB" is represented by the subgroup $\langle\sigma^3\tau\rangle$. However, these two partially synchronous states "ABBA" and "AABB," differing only in a cyclic change of their indices, are actually the same in dynamics. Similarly, the partially synchronous states "ABAB" and "BABA" are also the same and are represented by the subgroup $\langle\sigma^2\rangle$. Given that two partially synchronous states are the same if they only differ from each other in a cyclic change of the oscillator indices, we may claim that each partially synchronous state is represented by one conjugacy class of subgroups of dihedral group D_N and thus the number of different partially synchronous states is determined by the number of conjugacy classes of subgroups of D_N. Usually, the conjugacy class is represented by one representative subgroup within it, such as $\overline{\langle\sigma\tau\rangle}$ and $\overline{\langle\sigma^2\rangle}$ in the above examples. In fact, the subgroups in the same conjugacy class $\overline{S}$ of D_N are connected by $\sigma^k S \sigma^{-k}$ with different k, where the conjugate operation on the regular N-polygon plays the role of rotating the polygon, which justifies the correspondence between the partially synchronous states in a ring of N coupled identical oscillators and the conjugacy classes of D_N.

In Tables I and II, we present the correspondence between the partially synchronous states and the conjugacy classes of D_N for $N = 12$ and $N = 15$, where the trivial subgroups $\{e\}$ (for the desynchronous state) and $\langle\sigma\rangle$ (for the completely synchronous state) are also included for completeness. Note that there is an exception $\overline{\langle\sigma^4, \sigma\tau\rangle}$ which suggests the partially synchronous state "ABCB." However, the first and the third oscillators are actually in the same environment, which requires "A" to be the same as "C" except for the bistability. In the last row of both tables, we also include the partially synchronous states to be identified in the following section through desynchronized short chains with appropriate boundary conditions.

III. METHODOLOGY AND RESULTS

A. Identifying partially synchronous states

Though conjugacy classes of subgroups in D_N help to classify all possible partially synchronous states for $(N)_\mathrm{p}$, they

TABLE I. Correspondence between the conjugate classes and partially synchronous states for $N = 12$. In the head column, s.g. stands for subgroups, c.c. stands for conjugacy classes, and p.s.s. stands for partially synchronous states.

s.g.	$\{e\}$	$\langle\tau\rangle$	$\langle\sigma\tau\rangle$	$\langle\sigma^6\rangle$	$\langle\sigma^6,\tau\rangle$	$\langle\sigma^6,\sigma\tau\rangle$	$\langle\sigma^4\rangle$	$\langle\sigma^4,\tau\rangle$	$\langle\sigma^4,\sigma\tau\rangle$	$\langle\sigma^3\rangle$	$\langle\sigma^3,\tau\rangle$	$\langle\sigma^2\rangle$	$\langle\sigma^2,\tau\rangle$	$\langle\sigma^2,\sigma\tau\rangle$	$\langle\sigma\rangle$	$\langle\sigma,\tau\rangle$
		$\langle\sigma^2\tau\rangle$	$\langle\sigma^3\tau\rangle$		$\langle\sigma^6,\sigma^2\tau\rangle$	$\langle\sigma^6,\sigma^3\tau\rangle$		$\langle\sigma^4,\sigma^2\tau\rangle$	$\langle\sigma^4,\sigma^3\tau\rangle$		$\langle\sigma^3,\sigma\tau\rangle$					
		$\langle\sigma^4\tau\rangle$	$\langle\sigma^5\tau\rangle$		$\langle\sigma^6,\sigma^4\tau\rangle$	$\langle\sigma^6,\sigma^5\tau\rangle$					$\langle\sigma^3,\sigma^2\tau\rangle$					
		$\langle\sigma^6\tau\rangle$	$\langle\sigma^7\tau\rangle$													
		$\langle\sigma^8\tau\rangle$	$\langle\sigma^9\tau\rangle$													
		$\langle\sigma^{10}\tau\rangle$	$\langle\sigma^{11}\tau\rangle$													
c.c.	$\overline{\{e\}}$	$\overline{\langle\tau\rangle}$	$\overline{\langle\sigma\tau\rangle}$	$\overline{\langle\sigma^6\rangle}$	$\overline{\langle\sigma^6,\tau\rangle}$	$\overline{\langle\sigma^6,\sigma\tau\rangle}$	$\overline{\langle\sigma^4\rangle}$	$\overline{\langle\sigma^4,\tau\rangle}$	$\overline{\langle\sigma^4,\sigma\tau\rangle}$	$\overline{\langle\sigma^3\rangle}$	$\overline{\langle\sigma^3,\tau\rangle}$	$\overline{\langle\sigma^2\rangle}$	$\overline{\langle\sigma^2,\tau\rangle}$	$\overline{\langle\sigma^2,\sigma\tau\rangle}$	$\overline{\langle\sigma\rangle}$	$\overline{\langle\sigma,\tau\rangle}$
p.s.s.	$(12)_p$	$(7)_{nf}$	$(6)_o$	$(6)_p$	$(4)_{nf}$	$(3)_o$	$(4)_p$	N/A	$(2)_o$	$(3)_p$	$(2)_h$	$(2)_p \cong$	$(2)_{nf}$	$(1)_o \cong$	$(1)_p \cong$	$(1)_h$

do not reveal details about the dynamics and the stabilities of these states. In the following, we propose another effective recipe to find all partially synchronous states in $(N)_p$. It turns out that the partially synchronous dynamics in $(N)_p$ on their synchronous manifolds can be identified by categorizing short chains with end oscillators obeying various types of boundary conditions.

First, we identify all partially synchronous states represented by $\overline{\langle\sigma^m\rangle}$ with m the factor of N. If N is a prime number, then apparently no such partially synchronous state exists. Otherwise, if m is a proper factor, then the state $\overline{\langle\sigma^m\rangle}$ exists and is invariant under the rotation operation σ^m. Correspondingly, the synchronous manifold is constrained by $\mathbf{x}_i(t) = \mathbf{x}_{i+m}(t)$ with $i \in \{1, \cdots, N\}$. Substituting these constrains into model (1), we find that the partially synchronous dynamics on the synchronous manifold is described by a short ring of m oscillators $(m)_p$,

$$\dot{\mathbf{x}}_i = \mathbf{F}(\mathbf{x}_i) + \epsilon[\mathbf{H}(\mathbf{x}_{i+1}) + \mathbf{H}(\mathbf{x}_{i-1}) - 2\mathbf{H}(\mathbf{x}_i)], \tag{2}$$

with $i \in \{1, \cdots, m\}$. If all oscillators in the short chain $(m)_p$ happen to be desynchronized, then the states in the original $(N)_p$ must correspond to the irreducible partially synchronous state $\overline{\langle\sigma^m\rangle}$. Traditionally, synchronization usually refers to the unison between time-dependent dynamical behaviors of oscillators. Here, we generalize the concept of synchronization by defining dynamical behaviors to be synchronous ones provided that the behaviors can be realized on the synchronous manifold. In this sense, synchronous states can even be time-independent ones.

The rest of partially synchronous states in $(N)_p$ possess reflection symmetry and they may be singled out by starting from partially synchronous states $\langle\sigma^m\rangle$ with $m > 2$. For even m, the subgroups $\langle\sigma^m, \sigma\tau\rangle$ and $\langle\sigma^m, \tau\rangle$ are not conjugate

TABLE II. Correspondence between the conjugate classes and partially synchronous states for $N = 15$. In the head column, s.g. stands for subgroups, c.c. stands for conjugacy classes, and p.s.s. stands for partially synchronous states.

s.g.	$\{e\}$	$\langle\tau\rangle$	$\langle\sigma^5\rangle$	$\langle\sigma^5,\tau\rangle$	$\langle\sigma^3\rangle$	$\langle\sigma^3,\tau\rangle$	$\langle\sigma\rangle$	$\langle\sigma,\tau\rangle$
		$\langle\sigma\tau\rangle$		$\langle\sigma^5,\sigma\tau\rangle$		$\langle\sigma^3,\sigma\tau\rangle$		
		$\langle\sigma^2\tau\rangle$		$\langle\sigma^5,\sigma^2\tau\rangle$		$\langle\sigma^3,\sigma^2\tau\rangle$		
		$\langle\sigma^3\tau\rangle$		$\langle\sigma^5,\sigma^3\tau\rangle$				
		$\langle\sigma^4\tau\rangle$		$\langle\sigma^5,\sigma^4\tau\rangle$				
c.c.	$\overline{\{e\}}$	$\overline{\langle\tau\rangle}$	$\overline{\langle\sigma^5\rangle}$	$\overline{\langle\sigma^5,\tau\rangle}$	$\overline{\langle\sigma^3\rangle}$	$\overline{\langle\sigma^3,\tau\rangle}$	$\overline{\langle\sigma\rangle}$	$\overline{\langle\sigma,\tau\rangle}$
p.s.s.	$(15)_p$	$(8)_h$	$(5)_p$	$(3)_h$	$(3)_p$	$(2)_h$	$(1)_p \cong$	$(1)_h$

and, therefore, the related partially synchronous states are different. For the former, the synchronous manifold is constrained by $\mathbf{x}_i(t) = \mathbf{x}_{m-i+2}(t)$ with $i \in \{1, \cdots, \frac{m}{2}+1\}$ in the short chain $(m)_p$. Substituting these constrains into Eq. (2), we have

$$\begin{aligned}
\dot{\mathbf{x}}_1 &= \mathbf{F}(\mathbf{x}_1) + 2\epsilon[\mathbf{H}(\mathbf{x}_2) - \mathbf{H}(\mathbf{x}_1)],\\
\dot{\mathbf{x}}_i &= \mathbf{F}(\mathbf{x}_i) + \epsilon[\mathbf{H}(\mathbf{x}_{i+1}) + \mathbf{H}(\mathbf{x}_{i-1}) - 2\mathbf{H}(\mathbf{x}_i)],\\
\dot{\mathbf{x}}_{\frac{m}{2}+1} &= \mathbf{F}\big(\mathbf{x}_{\frac{m}{2}+1}\big) + 2\epsilon\big[\mathbf{H}\big(\mathbf{x}_{\frac{m}{2}}\big) - \mathbf{H}\big(\mathbf{x}_{\frac{m}{2}+1}\big)\big].
\end{aligned} \tag{3}$$

That is, we get a short chain of $\frac{m}{2}+1$ identical oscillators with end oscillators 1 and $\frac{m}{2}+1$ subjected to no-flux boundary conditions and we denote the chain by $(\frac{m}{2}+1)_{nf}$. The desynchronized $(\frac{m}{2}+1)_{nf}$ then gives rise to the dynamics of partially synchronous state $\overline{\langle\sigma^m, \sigma\tau\rangle}$ of $(N)_p$ on its synchronous manifold. For the latter, its synchronous manifold requires $\mathbf{x}_i(t) = \mathbf{x}_{m-i+1}(t)$ with $i \in \{1, \cdots, \frac{m}{2}\}$ and, consequently, Eq. (2) yields a chain of $\frac{m}{2}$ oscillators with open boundary conditions, denoted as $(\frac{m}{2})_o$ and obeying

$$\begin{aligned}
\dot{\mathbf{x}}_1 &= \mathbf{F}(\mathbf{x}_1) + \epsilon[\mathbf{H}(\mathbf{x}_2) - \mathbf{H}(\mathbf{x}_1)],\\
\dot{\mathbf{x}}_i &= \mathbf{F}(\mathbf{x}_i) + \epsilon[\mathbf{H}(\mathbf{x}_{i+1}) + \mathbf{H}(\mathbf{x}_{i-1}) - 2\mathbf{H}(\mathbf{x}_i)],\\
\dot{\mathbf{x}}_{\frac{m}{2}} &= \mathbf{F}\big(\mathbf{x}_{\frac{m}{2}}\big) + \epsilon\big[\mathbf{H}\big(\mathbf{x}_{\frac{m}{2}-1}\big) - \mathbf{H}\big(\mathbf{x}_{\frac{m}{2}}\big)\big].
\end{aligned} \tag{4}$$

Similarly, desynchronized $(\frac{m}{2})_o$ yields the partially synchronous state $\overline{\langle\sigma^m, \tau\rangle}$ of $(N)_p$.

However, for odd m, the subgroups $\langle\sigma^m, \tau\rangle$ and $\langle\sigma^m, \sigma\tau\rangle$ are conjugate and therefore, $\overline{\langle\sigma^m, \tau\rangle}$ and $\overline{\langle\sigma^m, \sigma\tau\rangle}$ represent the same states. The synchronous manifold requires $\mathbf{x}_i(t) = \mathbf{x}_{m+2-i}(t)$ with $i \in \{1, \cdots, \frac{m+1}{2}\}$, which leads to a chain of $\frac{m+1}{2}$ oscillators

$$\begin{aligned}
\dot{\mathbf{x}}_1 &= \mathbf{F}(\mathbf{x}_1) + 2\epsilon[\mathbf{H}(\mathbf{x}_2) - \mathbf{H}(\mathbf{x}_1)],\\
\dot{\mathbf{x}}_i &= \mathbf{F}(\mathbf{x}_i) + \epsilon[\mathbf{H}(\mathbf{x}_{i+1}) + \mathbf{H}(\mathbf{x}_{i-1}) - 2\mathbf{H}(\mathbf{x}_i)],\\
\dot{\mathbf{x}}_{\frac{m+1}{2}} &= \mathbf{F}\big(\mathbf{x}_{\frac{m+1}{2}}\big) + \epsilon\big[\mathbf{H}\big(\mathbf{x}_{\frac{m-1}{2}}\big) - \mathbf{H}\big(\mathbf{x}_{\frac{m+1}{2}}\big)\big].
\end{aligned} \tag{5}$$

Note here the end oscillators 1 and $\frac{m+1}{2}$ obey the no-flux and the open boundary conditions, respectively. Accordingly, we classify the chain as the one with hybrid boundary conditions and denote it as $(\frac{m+1}{2})_h$. Likewise, the desynchronized $(\frac{m+1}{2})_h$ describes the partially synchronous states $\overline{\langle\sigma^m, \tau\rangle} \equiv \overline{\langle\sigma^m, \sigma\tau\rangle}$ of $(N)_p$.

B. Stability analysis

According to the above recipe, all partially synchronous dynamics on their synchronous manifolds in model (1) can be obtained from Eqs. (2)–(5). However, whether these states can be realized depends on the transverse stabilities of their synchronous dynamics. For $\overline{\langle\sigma^m\rangle}$ described by Eq. (2), if we treat any m adjacent oscillators as a super-oscillator in $(N)_\mathrm{p}$, their transverse stabilities can be analyzed by following the formulation for the completely synchronous states [9,10]

$$\begin{aligned}\delta\dot{\mathbf{x}}_i &= \mathbf{DF}(\mathbf{x}_i)\delta\mathbf{x}_i + \epsilon[\mathbf{DH}(\mathbf{x}_{i+1})\delta\mathbf{x}_{i+1}\\ &\quad + \mathbf{DH}(\mathbf{x}_{i-1})\delta\mathbf{x}_{i-1} - 2\mathbf{DH}(\mathbf{x}_i)\delta\mathbf{x}_i]\\ &\quad + \delta_{i,1}(e^{-i2\pi k/l} - 1)\mathbf{DH}(\mathbf{x}_m)\delta\mathbf{x}_m\\ &\quad + \delta_{i,m}(e^{i2\pi k/l} - 1)\mathbf{DH}(\mathbf{x}_1)\delta\mathbf{x}_1, \end{aligned} \tag{6}$$

where $i \in \{1, \cdots, m\}$ and $l = N/m$. $\delta_{i,1}$ and $\delta_{i,m}$ are the Kronecker-δ functions while $\mathbf{DF}$ and $\mathbf{DH}$ are the Jacobians of the functions $\mathbf{F}$ and $\mathbf{H}$. If the largest transverse Lyapunov exponents Λ calculated from Eqs. (2) and (6) for all $k \in \{1, \cdots, l-1\}$ are negative, then the partially synchronous state $\overline{\langle\sigma^m\rangle}$ is transversely stable.

For partially synchronous states $\overline{\langle\sigma^m, \tau\rangle}$ and $\overline{\langle\sigma^m, \sigma\tau\rangle}$ to be stable, a two-step transverse stability analysis is indispensable. In the first step, $\overline{\langle\sigma^m, \tau\rangle}$ and $\overline{\langle\sigma^m, \sigma\tau\rangle}$ should be transversely stable in the chain $(m)_\mathrm{p}$, which can be determined by transversally perturbing the dynamics described by Eqs. (3)–(5). In the second step, the realizations of $\overline{\langle\sigma^m, \tau\rangle}$ and $\overline{\langle\sigma^m, \sigma\tau\rangle}$ in $(m)_\mathrm{p}$ should be transversely stable in the original $(N)_\mathrm{p}$ with the largest transverse Lyapunov exponent determined by Eq. (6).

Now, we present the transverse stability analysis of the states $\overline{\langle\sigma^m, \tau\rangle}$ and $\overline{\langle\sigma^m, \sigma\tau\rangle}$ in the first step. For even $m > 2$, the subgroups $\langle\sigma^m, \sigma\tau\rangle$ and $\langle\sigma^m, \tau\rangle$ are not conjugate and therefore the related partially synchronous states are different. For the former ($\overline{\langle\sigma^m, \sigma\tau\rangle}$), the synchronous manifold is constrained by $\mathbf{x}_i(t) = \mathbf{x}_{m-i+2}(t)$ with $i \in \{1, \cdots, \frac{m}{2}+1\}$ in the short chain $(m)_\mathrm{p}$ and the dynamics on the synchronous manifold is described by $(\frac{m}{2}+1)_\mathrm{nf}$. Then we transversely perturb the state and let $\delta\mathbf{x}_i = \mathbf{x}_i(t) - \mathbf{x}_{m-i+2}(t)$ with $i \in \{1, \cdots, \frac{m}{2}+1\}$. Clearly, $\delta\mathbf{x}_1 = \delta\mathbf{x}_{\frac{m}{2}+1} = 0$ and the rest of perturbations evolve as

$$\begin{aligned}\delta\dot{\mathbf{x}}_2 &= \mathbf{DF}(\mathbf{x}_2)\delta\mathbf{x}_2 + \epsilon[\mathbf{DH}(\mathbf{x}_3)\delta\mathbf{x}_3 - 2\mathbf{DH}(\mathbf{x}_2)\delta\mathbf{x}_2],\\ \delta\dot{\mathbf{x}}_i &= \mathbf{DF}(\mathbf{x}_i)\delta\mathbf{x}_i + \epsilon[\mathbf{DH}(\mathbf{x}_{i+1})\delta\mathbf{x}_{i+1} + \mathbf{DH}(\mathbf{x}_{i-1})\delta\mathbf{x}_{i-1} - 2\mathbf{DH}(\mathbf{x}_i)\delta\mathbf{x}_i],\ i \in \left\{3, \cdots, \frac{m}{2}-2\right\},\\ \delta\dot{\mathbf{x}}_{\frac{m}{2}-1} &= \mathbf{DF}\big(\mathbf{x}_{\frac{m}{2}-1}\big)\delta\mathbf{x}_{\frac{m}{2}-1} + \epsilon\big[\mathbf{DH}\big(\mathbf{x}_{\frac{m}{2}-2}\big)\delta\mathbf{x}_{\frac{m}{2}-2} - 2\mathbf{DH}\big(\mathbf{x}_{\frac{m}{2}-1}\big)\delta\mathbf{x}_{\frac{m}{2}-1}\big].\end{aligned} \tag{7}$$

Together with Eq. (3), the largest transverse Lyapunov exponent Λ can be calculated. Negative Λ suggests the state to be transversely stable in the chain $(m)_\mathrm{p}$.

For the latter ($\langle\sigma^m, \tau\rangle$), the synchronous manifold requires $\mathbf{x}_i(t) = \mathbf{x}_{m-i+1}(t)$ with $i \in \{1, \cdots, \frac{m}{2}\}$. Then we perturb the synchronous dynamics and the evolution of disturbances $\delta\mathbf{x}_i = \mathbf{x}_i(t) - \mathbf{x}_{m-i+1}(t)$ is described by

$$\begin{aligned}\delta\dot{\mathbf{x}}_1 &= \mathbf{DF}(\mathbf{x}_1)\delta\mathbf{x}_1 + \epsilon[\mathbf{DH}(\mathbf{x}_2)\delta\mathbf{x}_2 - 3\mathbf{DH}(\mathbf{x}_1)\delta\mathbf{x}_1],\\ \delta\dot{\mathbf{x}}_i &= \mathbf{DF}(\mathbf{x}_i)\delta\mathbf{x}_i + \epsilon[\mathbf{DH}(\mathbf{x}_{i+1})\delta\mathbf{x}_{i+1} + \mathbf{DH}(\mathbf{x}_{i-1})\delta\mathbf{x}_{i-1} - 2\mathbf{DH}(\mathbf{x}_i)\delta\mathbf{x}_i],\ i \in \left\{2, \cdots, \frac{m}{2}-1\right\},\\ \delta\dot{\mathbf{x}}_{\frac{m}{2}} &= \mathbf{DF}\big(\mathbf{x}_{\frac{m}{2}}\big)\delta\mathbf{x}_{\frac{m}{2}} + \epsilon\big[\mathbf{DH}\big(\mathbf{x}_{\frac{m}{2}-1}\big)\delta\mathbf{x}_{\frac{m}{2}-1} - 3\mathbf{DH}\big(\mathbf{x}_{\frac{m}{2}}\big)\delta\mathbf{x}_{\frac{m}{2}}\big].\end{aligned} \tag{8}$$

Together with Eq. (4), the largest transverse Lyapunov exponent Λ can be calculated and negative Λ singles out the state transversely stable in the chain $(m)_\mathrm{p}$.

For odd m, the partially synchronous states $\overline{\langle\sigma^m, \sigma\tau\rangle}$ and $\overline{\langle\sigma^m, \tau\rangle}$ are the same. The synchronous manifolds for these states satisfy $\mathbf{x}_i(t) = \mathbf{x}_{m+2-i}(t)$ with $i \in \{1, \cdots, \frac{m+1}{2}\}$ and the transverse disturbances $\delta\mathbf{x}_i(t) = \mathbf{x}_i(t) - \mathbf{x}_{m+2-i}(t)$ evolve according to

$$\begin{aligned}\delta\dot{\mathbf{x}}_2 &= \mathbf{DF}(\mathbf{x}_2)\delta\mathbf{x}_2 + \epsilon[\mathbf{DH}(\mathbf{x}_3)\delta\mathbf{x}_3 - 2\mathbf{DH}(\mathbf{x}_2)\delta\mathbf{x}_2],\\ \delta\dot{\mathbf{x}}_i &= \mathbf{DF}(\mathbf{x}_i)\delta\mathbf{x}_i + \epsilon[\mathbf{DH}(\mathbf{x}_{i+1})\delta\mathbf{x}_{i+1} + \mathbf{DH}(\mathbf{x}_{i-1})\delta\mathbf{x}_{i-1} - 2\mathbf{DH}(\mathbf{x}_i)\delta\mathbf{x}_i],\ i \in \left\{3, \cdots, \frac{m-1}{2}\right\},\\ \delta\dot{\mathbf{x}}_{\frac{m+1}{2}} &= \mathbf{DF}\big(\mathbf{x}_{\frac{m+1}{2}}\big)\delta\mathbf{x}_{\frac{m+1}{2}} + \epsilon\big[\mathbf{DH}\big(\mathbf{x}_{\frac{m-1}{2}}\big)\delta\mathbf{x}_{\frac{m-1}{2}} - 3\mathbf{DH}\big(\mathbf{x}_{\frac{m+1}{2}}\big)\delta\mathbf{x}_{\frac{m+1}{2}}\big].\end{aligned} \tag{9}$$

Together with Eq. (5), the largest transverse Lyapunov exponent Λ can be calculated and negative Λ distinguishes the state transversely stable in the chain $(m)_\mathrm{p}$.

C. Numerical simulation

1. Lorenz oscillator

To check the above theory, we set $N = 6$ and set local dynamics to be the Lorenz oscillator, i.e., $\mathbf{F}(\mathbf{x}) = [\sigma(y - x), rx - y - xz, xy - \beta z]$ with $\sigma = 10$, $r = 28$, and $\beta = 1$. The coupling function is taken to be $\mathbf{H}(\mathbf{x}) = (y, 0, 0)$. For this type of coupling function, complete synchronization is not possible for large N, and for small N it requires an intermediate coupling strength. To investigate the partially synchronous states, we numerically simulate Eq. (1) using the fourth order Runge-Kutta algorithm with time step $\Delta t = 0.01$. The first four largest Lyapunov exponents of the coupled oscillators are presented in Figs. 1(a) and 1(b) for the forward and backward continuations, respectively. In the forward (backward) continuation, the initial conditions of all oscillators for the

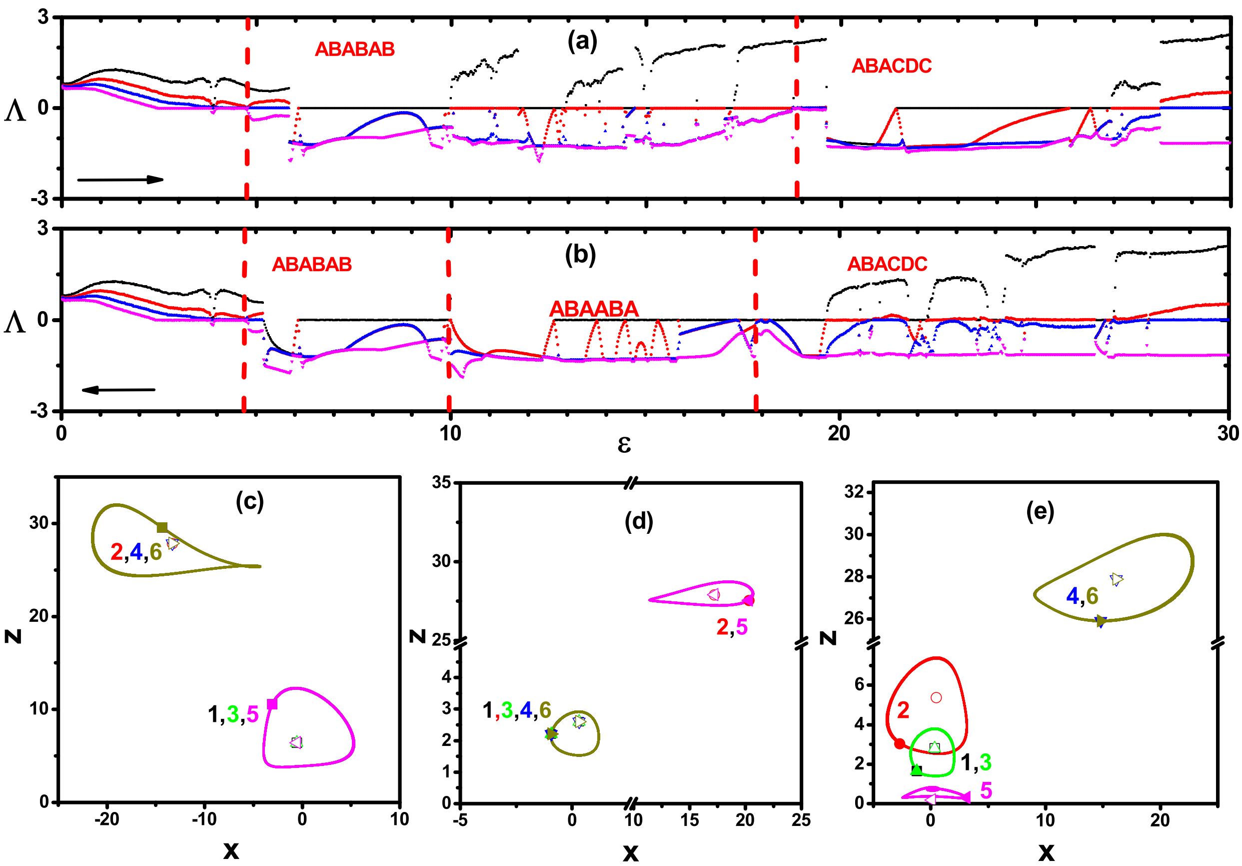

FIG. 1. Simulation of coupled identical Lorenz oscillators with $\sigma = 10$, $r = 28$, $\beta = 1$, and $N = 6$. The first four largest Lyapunov exponents against the coupling strength ϵ for the forward continuation in panel (a) and the backward continuation in panel (b); the trajectories of oscillators in the x-z plane for equilibria "ABABAB" (open symbols) at $\epsilon = 5.8$ and periodic "ABABAB" (solid symbols) at $\epsilon = 12$ in panel (c), equilibria "ABAABA" at $\epsilon = 12$ and periodic "ABAABA" at $\epsilon = 13$ in panel (d), equilibria "ABACDC" at $\epsilon = 20$ and periodic "ABACDC" at $\epsilon = 23$ in panel (e). The vertical dash lines in panels (a) and (b) denote the boundaries of stability diagrams of different partially synchronous states "ABABAB," "ABACDC," and "ABAABA." The locations of these dashed lines are numerically obtained by reading the final states of oscillators in the forward and the backward continuations. The numbers 1–6 in different colors in panels (c–e) indicate the positions of oscillators 1-6 at an arbitrary instant.

first parameter set are randomly assigned. Then, the coupling strength is increased (decreased) with $\Delta\epsilon = 0.02$ and the final states of the model are used as initial conditions for the next coupling strength. By monitoring the dynamics such as the phase portraits and time series, we can identify three types of partially synchronous states, "ABABAB," "ABACDC," and "ABAABA," whose stability regimes are depicted in Figs. 1(a) and 1(b). As shown, different *stable* partially synchronous states may coexist at the same coupling strength. To get more information on the dynamics of these partially synchronous states, we consider their trajectories in the x-z plane and the snapshots of oscillators. Figure 1(c) shows the equilibrium "ABABAB" at $\epsilon = 5.8$ and the periodic "ABABAB" at $\epsilon = 12$. As shown, six oscillators organize themselves into two groups and oscillators in the same group are in complete synchronization. Furthermore, the state "ABACDC" contains four different trajectories in Fig. 1(d) and the state "ABAABA" contains two different trajectories in Fig. 1(e). Different from the phase-locked states determined by the H/K theorem where all oscillators are in the same orbit [24,25], the partially synchronous states in this work may contain different trajectories and oscillators in the same group are in complete synchronization.

Moreover, different modules are recognized in building up the patterns of these partially synchronous states. For example, the module "AB" in "ABABAB," and the module "BACD" in "ABACDC." For the state "ABAABA," there are two modules "ABA" and "AB" at different levels. These modules form partially synchronous states through the symmetrical operations of the rotation and the reflection.

The analysis on the conjugacy classes of subgroups of D_6 gives rise to five possible partially synchronous states in model (1) with $N = 6$, $\overline{\langle\sigma^2\rangle}$ represented by "ABABAB," $\overline{\langle\sigma^3\rangle}$ by"ABCABC," $\overline{\langle\sigma^3, \tau\rangle}$ by "ABAABA," $\overline{\langle\tau\rangle}$ by "ABCCBA," and $\overline{\langle\sigma\tau\rangle}$ by "ABACDC." The dynamics of these states on their synchronous manifolds can be determined by investigating the short chains, $(2)_\mathrm{p}$, $(3)_\mathrm{p}$, $(2)_\mathrm{h}$, $(3)_\mathrm{o}$, and $(4)_\mathrm{nf}$, and whether they can be realized depends on their transverse stabilities. In Fig. 2(a), we show the bifurcation diagram of the short chain $(2)_\mathrm{p}$ where the largest transverse Lyapunov exponent Λ is color-encoded with red (green) denoting $\Lambda < 0$ ($\Lambda > 0$). We define the departure between oscillators as

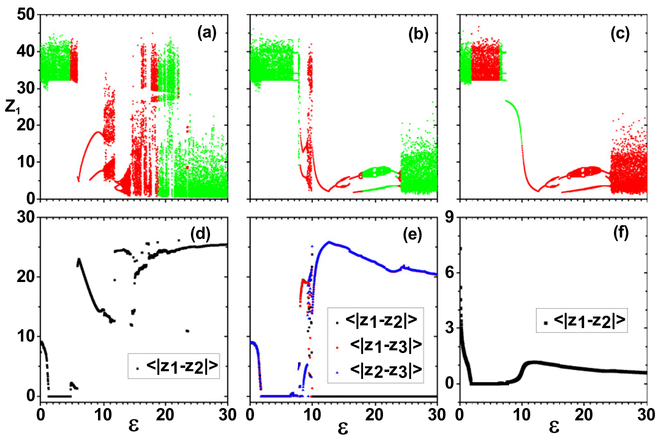

FIG. 2. Simulation of coupled identical Lorenz oscillators with $\sigma = 10$, $r = 28$, $\beta = 1$, and $N = 6$. The bifurcation diagrams for the chain $(2)_\mathrm{p}$ in panel (a), $(3)_\mathrm{p}$ in panel (b), and $(2)_\mathrm{h}$ in panel (c) with red (green) denoting the largest transverse Lyapunov exponent $\Lambda < 0$ ($\Lambda > 0$). The departures between oscillator pairs for the chain $(2)_\mathrm{p}$ in panel (d), $(3)_\mathrm{p}$ in panel (e), and $(2)_\mathrm{h}$ in panel (f).

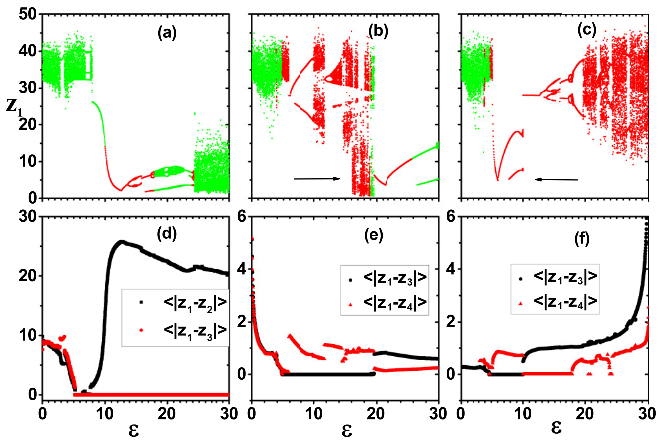

FIG. 3. Simulation of coupled identical Lorenz oscillators with $\sigma = 10$, $r = 28$, $\beta = 1$, and $N = 6$. The bifurcation diagrams for the chain $(3)_\mathrm{o}$ in panel (a), $(4)_\mathrm{nf}$ with forward continuation in panel (b), and $(4)_\mathrm{nf}$ with backward continuation in panel (c) with red (green) denoting the largest transverse Lyapunov exponent $\Lambda < 0$ ($\Lambda > 0$). The departures between oscillator pairs for the chain $(3)_\mathrm{o}$ in panel (d), $(4)_\mathrm{nf}$ with forward continuation in panel (e), and $(4)_\mathrm{nf}$ with backward continuation in panel (f).

$\langle |z_1 - z_2| \rangle$ with $\langle \cdot \rangle$ designating the time average. As shown in Fig. 2(d), the chain $(2)_\mathrm{p}$ supports the synchronous state "AA" ($\langle |z_1 - z_2| \rangle = 0$) and the desynchronous state "AB" ($\langle |z_1 - z_2| \rangle \neq 0$). The former corresponds to the complete synchronization in $(6)_\mathrm{p}$ while the latter to the state "ABABAB." As shown in Figs. 2(a) and 2(d), the state "ABABAB" is stable for $\epsilon \in (4.7, 19)$ while the complete synchronization is transversely unstable, which are in agreement with Fig. 1. For the chain $(3)_\mathrm{p}$, the bifurcation diagram with color-encoded Λ is presented in Fig. 2(b) while $\langle |z_i - z_j| \rangle$ are plotted in Fig. 2(e). As shown, the desynchronous state "ABC" in $(3)_\mathrm{p}$ is transversely stable for $\epsilon \in (8, 10)$ though its counterpart "ABCABC" in $(6)_\mathrm{p}$ is not observed in Fig. 1. Actually, the state "ABCABC" in $(6)_\mathrm{p}$ can be realized by numerically simulating model (1) with appropriate initial conditions. For the state "ABAABA" in $(6)_\mathrm{p}$, its dynamics on the synchronous manifold is described by the desynchronous state "AB" in the chain $(2)_\mathrm{h}$. As shown in Figs. 2(c) and 2(f), the state "AB' is transversely stable for $\epsilon \in (10, 30)$. However, the two-step stability of $\overline{\langle \sigma^3, \tau \rangle}$ requires further transverse stability of the state "AAB" in $(3)_\mathrm{p}$, which is satisfied for $\epsilon \in (10, 18)$ as shown in Figs. 2(b) and 2(e). Combining these two stability regimes together, we know that the state "ABAABA" in the chain $(6)_\mathrm{p}$ is transversely stable for $\epsilon \in (10, 18)$, which is consistent with Fig. 1.

Figures 3(a) and 3(d) show the results for the short chain $(3)_\mathrm{o}$. The desynchronous state "ABC" is transversely unstable and, correspondingly, the partially synchronous state "ABCCBA" ($\overline{\langle \sigma \tau \rangle}$) in $(6)_\mathrm{p}$ can not be realized. In contrast, the partially synchronous state "ABA" in $(3)_\mathrm{o}$ is transversely stable for $\epsilon \in (10, 18)$, which refers to the state "ABAABA" in the chain $(6)_\mathrm{p}$. For the short chain $(4)_\mathrm{nf}$ where the desynchronous state "BACD" refers to the partially synchronous state "ABACDC" in $(6)_\mathrm{p}$, we present the results for both forward and backward continuations in Figs. 3(b), 3(e) and Figs. 3(c), 3(f), respectively. As shown, the state "BACD" is transversely stable for $\epsilon \in (19.5, 25)$ in the forward continuation while in the backward continuation it is transversely stable for $\epsilon \in (18, 30)$. Note that the same partially synchronous states may allow for different dynamics even at the same coupling strength. For instance, both the periodic dynamics in Fig. 3(b) and the chaotic dynamics in Fig. 3(c) are displayed at $\epsilon = 24$ for the state "ABACDC."

2. Rössler oscillator

Now we consider the local dynamics to be the Rössler oscillator, i.e., $\mathbf{F}(\mathbf{x}) = [-y - z, x + ay, b + (x - c)z]$ with $a = 0.175$, $b = 0.4$, and $c = 8.5$. We set $N = 6$. The coupling function is taken to be $\mathbf{H}(\mathbf{x}) = (x, y, z)$, which has been already investigated in a different way in Ref. [15]. For this type of coupling function, the complete synchronization may be reached at around $\epsilon > 0.088$ for $N = 6$. Figures 4(a) and 4(b) show the first four largest Lyapunov exponents of the coupled oscillators for the forward and backward continuations, respectively. In these two bifurcation scenarios, we may identify four partially synchronous states, "ABCBAC," "ABAABA," "ABABAB," and "ABACDC," with their stability regimes being depicted in Figs. 4(a) and 4(b). Compared with the case of Lorenz oscillators, there exist large parameter regimes which do not support partially synchronous states. The trajectories of these partially synchronous states and the corresponding snapshots of oscillators are presented in the rest of Fig. 4. Interestingly, for certain partially synchronous states, all oscillators share a same trajectory on which oscillators keep a fixed phase difference between them, for which the H/K theorem might be applied. For example, the state "ABCBAC" at $\epsilon = 0.0052$ in Fig. 4(c) has adjacent oscillators with phase differences of $T/3$ on a period-3 trajectory with the period being T, while the state "ABABAB" at $\epsilon = 0.021$ in Fig. 4(e) has adjacent oscillators with phase differences of $T/2$ on a period-2 trajectory. However, for other two partially synchronous states, oscillators organize themselves into two

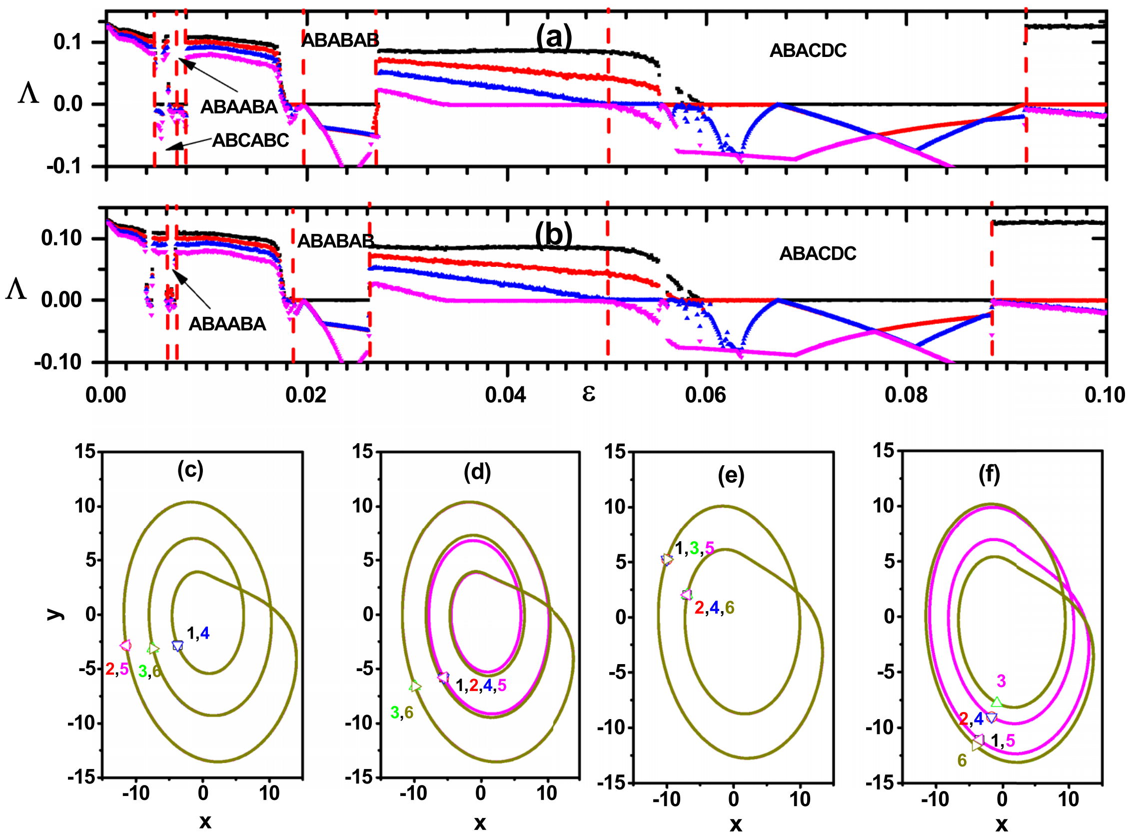

FIG. 4. Simulation of coupled identical Rössler oscillators with $a = 0.175$, $b = 0.4$, $c = 8.5$, and $N = 6$. The first four largest Lyapunov exponents against the coupling strength ϵ for the forward continuation in panel (a) and the backward continuation in panel (b); The trajectories of oscillators in the x-y plane for "ABCABC" at $\epsilon = 0.0052$ in panel (c), "ABAABA" at $\epsilon = 0.0075$ in panel (d), "ABABAB" at $\epsilon = 0.021$ in panel (e), and "ABACDC" at $\epsilon = 0.09$ in panel (f). The vertical dashed lines in panel (a, b) denote the boundaries of stability regimes of different partially synchronous states "ABCABC," "ABAABA," "ABABAB," and "ABACDC." The numbers 1–6 in different colors in panels (c–f) indicate the positions of oscillators 1–6 at an arbitrary instant.

groups and each group of oscillators share a same trajectory. Figure 4(d) shows the state "ABAABA" at $\epsilon = 0.021$. As shown, there are two groups of oscillators falling onto two different period-3 trajectories, one group consisting of four oscillators in the complete synchronization while the other consisting of only two synchronized oscillators. Figure 4(f) shows the state "ABACDC" at $\epsilon = 0.09$ where four oscillators fall onto one period-2 trajectory and two others onto the other period-2 trajectory. Note that in the state "ABACDC," each group of oscillators are further partitioned into two subgroups which have phase differences of $T/2$ on the period-2 trajectories.

Following the above protocol, the stabilities of possible partially synchronous states can be investigated by analyzing the transverse stability of the dynamics on the short chains, $(2)_\mathrm{p}$, $(3)_\mathrm{p}$, $(2)_\mathrm{h}$, $(3)_\mathrm{o}$, and $(4)_\mathrm{nf}$. Figure 5(a) shows $\langle|z_1 - z_2|\rangle$ against ϵ in the forward continuation where the largest transverse Lyapunov exponent Λ is color-encoded with red (green) denoting $\Lambda < 0$ ($\Lambda > 0$). As shown, the desynchronous state "AB" ($\langle|z_1 - z_2|\rangle \neq 0$), denoting the state "ABABAB," is transversely stable in the range $\epsilon \in (0.019, 0.027)$, which is compatible with Fig. 4. Similarly, we can identify the state "ABCBAC" with all $\langle|z_i - z_j|\rangle$ being nonzero in $(3)_\mathrm{o}$ [Fig. 5(b)], the state "ABAABA" with nonzero $\langle|z_1 - z_2|\rangle$ in $(2)_\mathrm{h}$ [Fig. 5(c)], the state "ABCCBA" with all $\langle|z_i - z_j|\rangle$ being nonzero in $(3)_\mathrm{o}$ [Fig. 5(d)], and the state "ABACDC" with nonzero $\langle|z_1 - z_3|\rangle$ and $\langle|z_1 - z_4|\rangle$ in $(4)_\mathrm{nf}$ [Fig. 5(e)]. In comparison with Fig. 4, we find that the analyses on the transverse stabilities of the dynamics on the short chains provide more accurate information on the stability regimes of partially synchronous states, for example the existence of stable "ABCABC" at around $\epsilon \in (0.022, 0.025)$ [see Fig. 5(b)] and stable "ABCCBA" at large ϵ [see Fig. 5(d)], which are not observed in Fig. 4.

D. Hierarchy of partially synchronous states

The recipe proposed above suggests a hierarchical organization of partially synchronous states in $(N)_\mathrm{p}$, which is essentially the inclusion relation among subgroups of D_N. Take the partially synchronous states $\overline{\langle\sigma^m\rangle}$ and $\overline{\langle\sigma^m, \tau\rangle}$ as an example. The inclusion relation $\langle\sigma^m\rangle \subset \langle\sigma^m, \tau\rangle$ indicates that we may obtain $\overline{\langle\sigma^m, \tau\rangle}$ by enforcing extra reflection symmetry to the state $\overline{\langle\sigma^m\rangle}$. Likewise, $\overline{\langle\sigma^m, \tau\rangle}$ may give rise to $\overline{\langle\sigma^{m/2}, \tau\rangle}$ for even m due to $\langle\sigma^m\rangle \subset \langle\sigma^{m/2}, \tau\rangle$. Using the inclusion relations among subgroups of D_N as directed links, partially synchronous states of $(N)_\mathrm{p}$ organize themselves into a hierarchical network. In Fig. 6, we draw the hierarchical networks for $N = 12$ and $N = 15$, where the nodes refer to the partially synchronous states (conjugacy classes) and the directed links

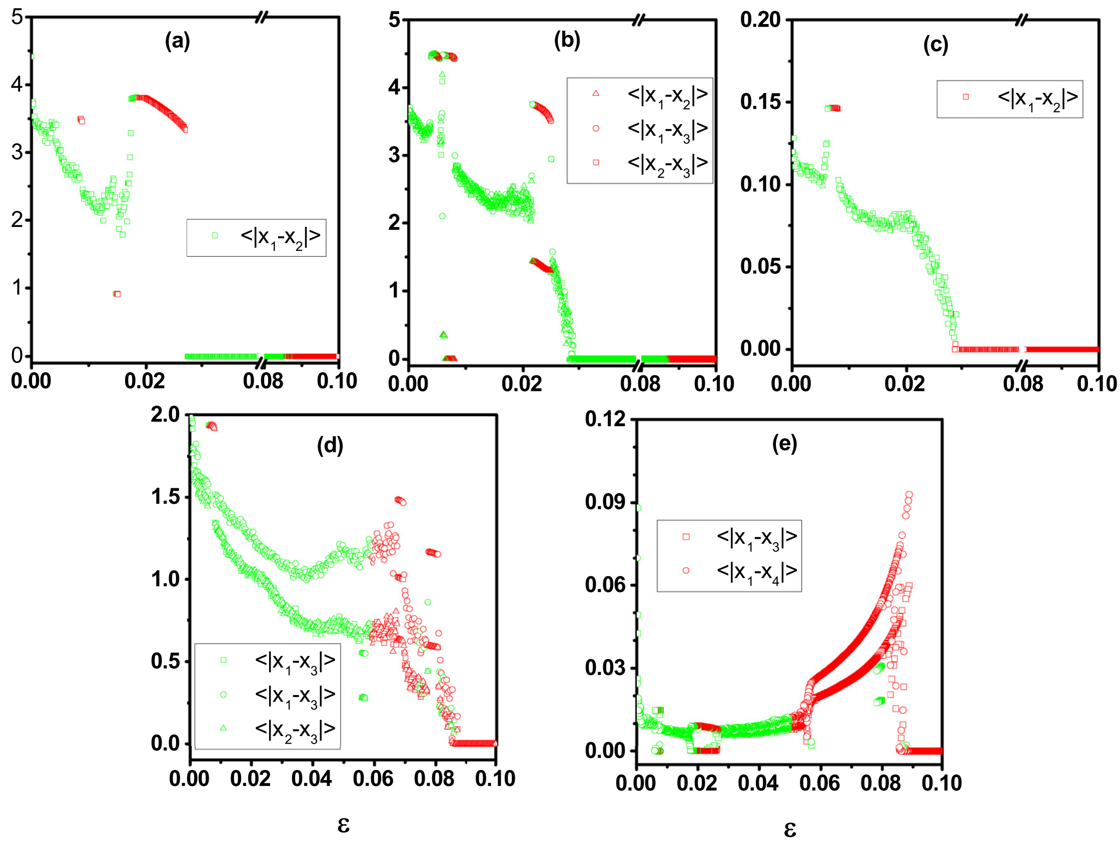

FIG. 5. Simulation of coupled identical Rössler oscillators with $a = 0.175$, $b = 0.4$, $c = 8.5$, and $N = 6$. The departures between oscillator pairs, $\langle |z_i - z_j| \rangle$, for the chain $(2)_\mathrm{p}$ in panel (a), $(3)_\mathrm{p}$ in panel (b), $(2)_\mathrm{h}$ in panel (c), $(3)_\mathrm{o}$ in panel (d), and $(4)_\mathrm{nf}$ in panel (e).

show the inclusion relations between states. We include the desynchronous state $\overline{\{e\}}$, as well as the complete synchronous state $\overline{\langle\sigma\rangle}$, in the network. For clarity, the direct inclusion relation between two conjugacy classes is not shown if there exist paths between them with the path length larger than 1. The short chains with distinct boundary conditions, which represent the dynamics of the corresponding partially synchronous states on their synchronous manifolds, are also included as the subscripts. Calibrating the degree of synchronization for partially synchronous states as the maximum number of oscillators in the same synchronous cluster, the hierarchical network clearly shows that downstream partially synchronous states are more synchronous than the upstream ones. Additionally, due to the correspondence between the partially synchronous states and desynchronized short chains, it is obvious that, along directed paths, chains describing partially synchronous states get shorter and shorter. In other words, downstream short chains with various boundary conditions can be obtained from upstream chains after suitable symmetry considerations. Take, for example, the path $\overline{\langle\sigma^6\rangle}_{(6)_\mathrm{p}} \rightarrow \overline{\langle\sigma^6, \tau\rangle}_{(4)_\mathrm{nf}} \rightarrow \overline{\langle\sigma^3, \tau\rangle}_{(2)_\mathrm{h}}$ in Fig. 6(a). In the chain $(6)_\mathrm{p}$, the state "ABCDEF" represents the dynamics of the partially synchronous state $\overline{\langle\sigma^6\rangle}$ on its synchronous manifold, "ABCDCB" the synchronous dynamics of $\overline{\langle\sigma^6, \tau\rangle}_{(4)_\mathrm{nf}}$, and "ABBABB" the synchronous dynamics of $\overline{\langle\sigma^3, \tau\rangle}_{(2)_\mathrm{h}}$. Actually, it is these downstream short chains that act as the modules in the pattern formation of partially synchronous states.

IV. CONCLUSIONS

In this work, we have proposed a general theory on the partially synchronous states in a ring of locally coupled identical oscillators. We related a partially synchronous state to a subgroup of the dihedral group D_N and classified partially synchronous states with conjugacy classes of the subgroups of D_N. We then provided a recipe to search for all possible partially synchronous dynamics by reducing a ring of oscillators to shorter chains of oscillators with different boundary conditions and presented a two-step transverse stability analysis on their dynamics on the synchronous manifold. Based on the theory, we found that the partially synchronous states organized themselves into a hierarchical network, which suggests the existence of modules in the pattern of partially synchronous states. Along directed paths in the network, down stream partially synchronous states are more synchronous than upstream ones. In addition, researchers always focused on coupled oscillators with periodic boundary conditions while chains of oscillators with other boundary conditions such as open or no-flux boundary conditions are seldom investigated [37]. However, as shown in this work, partial synchronization on a ring of coupled oscillators can be illustrated by investigating the dynamics on chains of oscillators, which also means that the partial synchronization in chains of identical oscillators with different boundary conditions can be solved by mapping them back to a ring of oscillators. The relation between the dynamics on a ring of oscillators

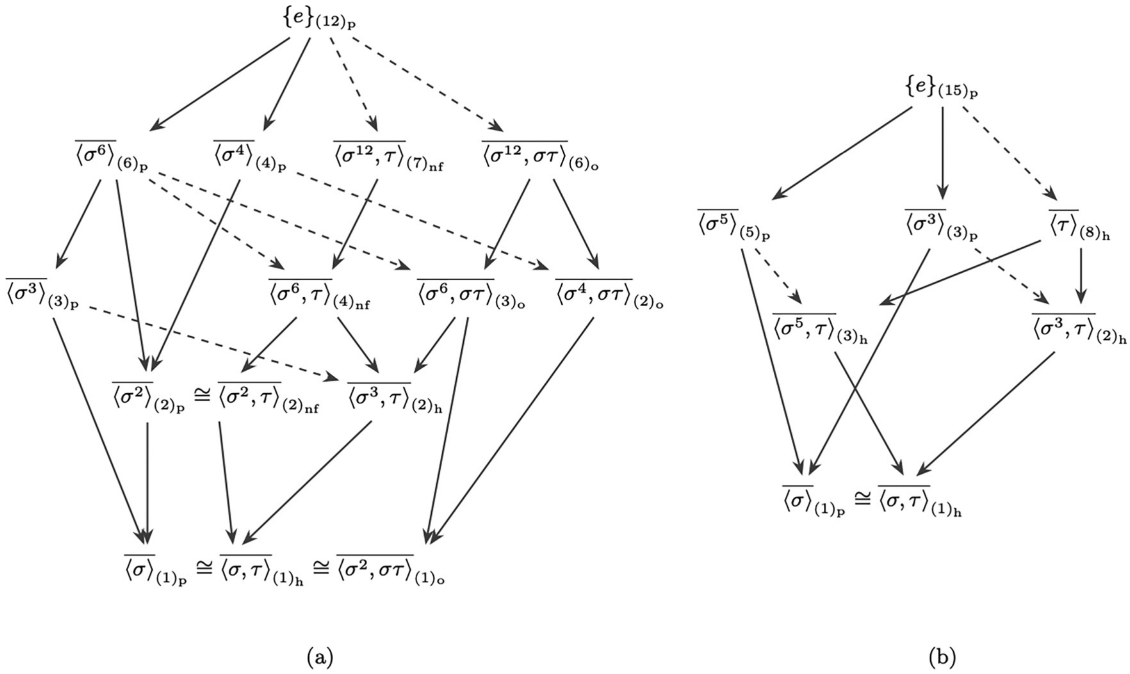

FIG. 6. The hierarchy of conjugate classes of subgroups of the dihedral groups and corresponding partially synchronous states for (a) $N = 12$ and (b) $N = 15$. The symbol $\cong$ denotes that two related conjugate classes, e.g., $\overline{\langle\sigma^2\rangle}_{(2)_p}$ and $\overline{\langle\sigma^2,\tau\rangle}_{(2)_{nf}}$, correspond to the same partially synchronous states. The arrow indicates that for any subgroup H in a conjugate class at the arrow tail, there exits a subgroup K in the conjugate class at the arrow head, which satisfies that H is contained in K. Meanwhile, it also indicates that the partial synchronization states at the arrow head are special cases of those at the arrow tail. Arrows with dashed lines explicitly distinguish connections from the partial synchronous states corresponding to conjugated classes of subgroups without the elementary reflection τ to the partial synchronous states corresponding to those with τ.

and on chains of oscillators is worth investigating in the future.

To be noted, the theory developed in this work applies to a model possessing the symmetry described by the dihedral group D_N and, therefore, cannot be exploited to classify partially synchronous states in complex networks. Nevertheless, the theory may be generalized to a ring of nonlocally coupled identical oscillators which also possessing D_N symmetry. In a ring of nonlocally coupled oscillators, the connection between partially synchronous states and the conjugacy classes of subgroups of D_N is the same. However, to search for all possible partially synchronous states and to investigate their transverse stabilities, Eqs. (3)–(9) have to be modified accordingly to be in more complicated form.

ACKNOWLEDGMENTS

This work is partly supported by the National Natural Science Foundation of China under Grant No. 11475021 and the National Key Basic Research Program of China under Grant No. 2013CB922000.

APPENDIX: BRIEFS ON THE DIHEDRAL GROUP D_N

The dihedral group D_N ($N \geqslant 3$) of order $2N$ is often called the group of symmetries of a regular N-polygon, which arises frequently in arts and nature. For example, Mercedes-Benz's logo has D_3 as a symmetry group and snowflakes have D_6 symmetry. The group D_N consists of $2N$ elements: $e, \sigma, \cdots, \sigma^{N-1}, \tau, \sigma\tau, \cdots, \sigma^{N-1}\tau$. The element σ^k ($k \in \{0, \cdots, N-1\}$) refers to a $2k\pi/N$ in-plane rotation about the center, and $\sigma^0 \equiv \sigma^N$ is the identity e. The element $\sigma^k\tau$ refers to a reflection with respect to an in-plane axis through the center. For a regular N-polygon, there are N reflection axes. For odd N, each reflection axis connects the midpoint of one side to the opposite vertex. For even N, $N/2$ reflection axes connect the midpoints of opposite sides and the other $N/2$ reflection axes connect opposite vertices. Once the reflection axis L of τ is specified, the reflection axis of $\sigma^k\tau$ can be acquired by rotating L through $2k\pi/N$ for odd N or $k\pi/N$ for even N. The actions of D_N on regular N-polygons with $N = 3$ and $N = 4$ are demonstrated in Figs. 7(a) and 7(b), respectively. For example, for the square denoted by its four vertices $[\mathbf{x}_1, \mathbf{x}_2, \mathbf{x}_3, \mathbf{x}_4]$, the action of σ on the square yields $[\mathbf{x}_4, \mathbf{x}_1, \mathbf{x}_2, \mathbf{x}_3]$, the reflection τ gives rise to $[\mathbf{x}_4, \mathbf{x}_3, \mathbf{x}_2, \mathbf{x}_1]$, and the combined operation $\sigma\tau$ produces $[\mathbf{x}_1, \mathbf{x}_4, \mathbf{x}_3, \mathbf{x}_2]$. All elements of D_N can be expressed as successive operations of σ or τ in some form, therefore σ and τ are called the two generators of D_N. In this regard, the dihedral group D_N is represented as $D_N = \langle\sigma, \tau | \sigma^N = \tau^2 = e, \tau\sigma\tau = \sigma^{-1}\rangle$.

If a subset S of D_N is itself a group under the operation of D_N, then S is called a subgroup of D_N. Obviously, the subset $\{e\}$ and D_N are two trivial subgroups of D_N. Besides, there are three types of nontrivial subgroups of D_N. The first type contains only rotation elements, which is the subgroup of the cyclic group $\langle\sigma\rangle$, and therefore is represented as $\langle\sigma^m\rangle$ with m being a proper factor of N. The second type contains only reflection elements except for the identity, and likewise

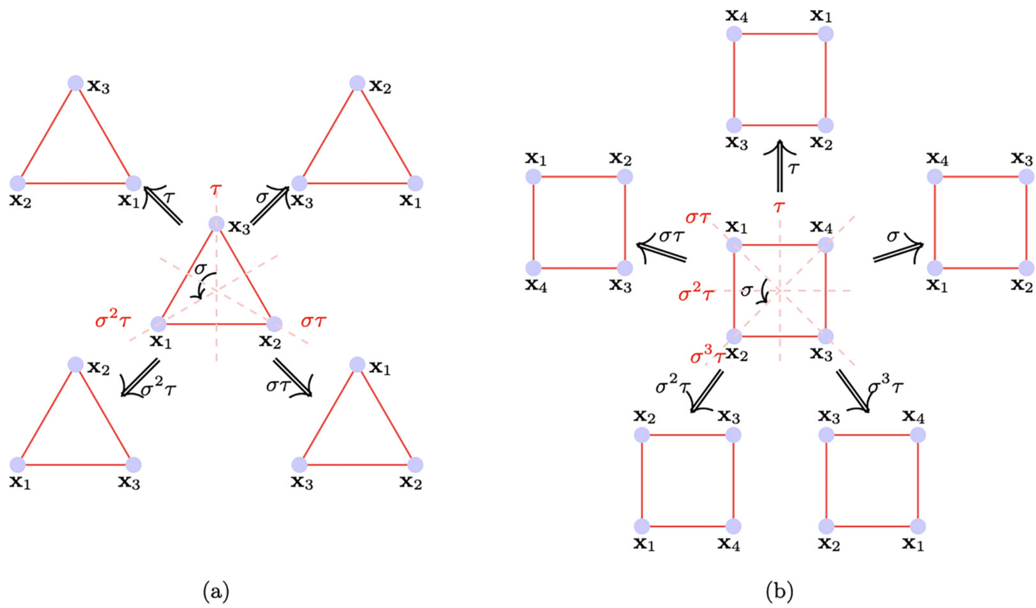

FIG. 7. The rotation and reflection operations on regular N-polygons for (a) $N = 3$, an equilateral triangle and (b) $N = 4$, a square. Although the labels of the reflection axes in red dashed lines are combinations of successive reflection and rotation operations, the reflection axes themselves are not supposed to be transformed through the elementary rotation from a particular reflection axis as the labels indicate.

is represented as $\langle\sigma^k\tau\rangle$ with $0 \leqslant k \leqslant N-1$. The third type contains not only rotation elements but also reflection ones, and so is represented as $\langle\sigma^m, \sigma^k\tau\rangle$ with m being a proper factor of N and $0 \leqslant k \leqslant m-1$.

The three types of subgroups may be organized into conjugacy classes of subgroups. Two subgroups S_1 and S_2 are conjugate if there exists one element $g \in D_N$ such that $S_1 = gS_2g^{-1}$ with g^{-1} being the inverse of g. Usually, the conjugacy class may be represented by one representative subgroup within it, such as $\overline{S}_1$ in the above example. It is clearly that subgroups $\langle\sigma^m\rangle$ with different m are not conjugate and the conjugacy class $\overline{\langle\sigma^m\rangle}$ contains only one subgroup. Observing that $\sigma^k\tau\sigma^{-k} = \sigma^{2k}\tau$, subgroups $\langle\sigma^k\tau\rangle$ are readily shown to belong to the same conjugacy class $\overline{\langle\tau\rangle}$ for odd N while two different conjugacy classes $\overline{\langle\tau\rangle}$ and $\overline{\langle\sigma\tau\rangle}$ for even N. Similarly, subgroups $\langle\sigma^m, \sigma^k\tau\rangle$ can be classified into different conjugacy classes, $\overline{\langle\sigma^m, \tau\rangle}$ and $\overline{\langle\sigma^m, \sigma\tau\rangle}$, according to the odevity of m.

[1] A. T. Winfree, *The Geometry of Biological Time* (Springer-Verlag, New York, 1980).

[2] H. Haken, *Synergetics: An Introduction* (Springer, Berlin, 1983).

[3] S. H. Strogatz, *Sync: The Emerging Science of Spontaneous Order* (Hyperion, New York, 2003).

[4] E. Tang and D. S. Bassett, Control of dynamics in brain networks, Rev. Mod. Phys. **90**, 031003 (2018).

[5] T. E. Lee and M. C. Cross, Pattern Formation with Trapped Ions, Phys. Rev. Lett. **106**, 143001 (2011).

[6] A. Pikovsky, M. Rosenblum, and J. Kurths, *Synchronization: A Universal Concept in Nonlinear Sciences* (Cambridge University Press, Cambridge, UK, 2001).

[7] G. Saxena, A. Prasad, and R. Ramaswamy, Amplitude death: The emergence of stationarity in coupled nonlinear systems, Phys. Rep. **521**, 205 (2012).

[8] M. Cross and H. Greenside, *Pattern Formation and Dynamics in Nonequilibrium Systems* (Cambridge University Press, Cambridge, UK, 2009).

[9] J. Yang, G. Hu, and J. Xiao, Chaos Synchronization in Coupled Chaotic Oscillators with Multiple Positive Lyapunov Exponents, Phys. Rev. Lett. **80**, 496 (1998).

[10] L. M. Pecora and T. L. Carroll, Master Stability Functions for Synchronized Coupled Systems, Phys. Rev. Lett. **80**, 2109 (1998).

[11] G. Hu, J. Yang, and W. Liu, Instability and controllability of linearly coupled oscillators: Eigenvalue analysis, Phys. Rev. E **58**, 4440 (1998).

[12] L. Huang, Q. Chen, Y. Lai, and L. M. Pecora, Generic behavior of master-stability functions in coupled nonlinear dynamical systems, Phys. Rev. E **80**, 036204 (2009).

[13] M. Barahona and L. M. Pecora, Synchronization in Small-World Systems, Phys. Rev. Lett. **89**, 054101 (2002).

[14] T. Nishikawa, A. E. Motter, Y. Lai, and F. C. Hoppensteadt, Heterogeneity in Oscillator Networks: Are Smaller Worlds Easier to Synchronize? Phys. Rev. Lett. **91**, 014101 (2003).

[15] Y. Zhang, G. Hu, H. A. Cerdeira, S. Chen, T. Braun, and Y. Yao, Partial synchronization and spontaneous spatial ordering in coupled chaotic systems, Phys. Rev. E **63**, 026211 (2001).

[16] A. Pikovsky, O. Popovych, and Yu. Maistrenko, Resolving Clusters in Chaotic Ensembles of Globally Coupled Identical Oscillators, Phys. Rev. Lett. **87**, 044102 (2001).

[17] G. Hu, Y. Zhang, H. A. Cerdeira, and S. Chen, From Low-Dimensional Synchronous Chaos to High-Dimensional

Desynchronous Spatiotemporal Chaos in Coupled Systems, Phys. Rev. Lett. **85**, 3377 (2000).
[18] B. Ao and Z. Zheng, Partial synchronization on complex networks, Europhys. Lett. **74**, 229 (2006).
[19] L. M. Pecora, F. Sorrentino, A. M. Hagerstrom, T. E. Murphy, and R. Roy, Cluster synchronization and isolated desynchronization in complex networks with symmetries, Nat. Commun. **5**, 4079 (2014).
[20] C. Fu, W. Lin, L. Huang, and X. Wang, Synchronization transition in networked chaotic oscillators: The viewpoint from partial synchronization, Phys. Rev. E **89**, 052908 (2014).
[21] L. Zhang, A. E. Motter, and T. Nishikawa, Incoherence-Mediated Remote Synchronization, Phys. Rev. Lett. **118**, 174102 (2017).
[22] A. Nazerian, S. Panahi, I. Leifer, D. Phillips, H. A. Makse, and F. Sorrentino, Matryoshka and disjoint cluster synchronization of networks, Chaos **32**, 041101 (2022).
[23] T. Menara, G. Baggio, D. Bassett, and F. Pasqualetti, Functional control of oscillator networks, Nat. Commun. **13**, 4721 (2022).
[24] M. Golubitsky and I. Stewart, Nonlinear Dynamics of networks: The groupoid formalism, Bull. Amer. Math. Soc. **43**, 305 (2006).
[25] M. Golubitsky, L. M. Messi, and L. E. Spardy, Symmetry types and phase-shift synchrony in networks, Physica D **320**, 9 (2016).
[26] I. Hunter, M. M. Norton, B. Chen, C. Simonetti, M. E. Moustaka, J. Touboul, and S. Fraden, Pattern formation in a four-ring reaction-diffusion network with heterogeneity, Phys. Rev. E **105**, 024310 (2022).
[27] I. Stewart and M. Parker, Periodic dynamics of coupled cell networks II: Cyclic symmetry, Dyn. Syst. **23**, 17 (2008).
[28] W. Poel, A. Zakharova, and E. Schöll, Partial synchronization and partial amplitude death in mesoscale network motifs, Phys. Rev. E **91**, 022915 (2015).
[29] W. Shuai and L. Yong, Synchronization or cluster synchronization in coupled Van der Pol oscillators networks with different topological types, Phys. Scr. **97**, 035205 (2022).
[30] A. Salova and R. M. D'Souza, Decoupled synchronized states in networks of linearly coupled limit cycle oscillators, Phys. Rev. Res. **2**, 043261 (2020).
[31] B. Fiedler, S. W. Haugland, F. P. Kemeth, and K. Krischer, Global heteroclinic rebel dynamics among large 2-clusters in permutation equivariant systems, SIAM J. Appl. Dyn. Syst. **20**, 1277 (2021).
[32] I. Schneider and M. Bosewitz, Eliminating restrictions of time-delayed feedback control using equivariance, Discrete Contin. Dyn. Syst. **36**, 451 (2016).
[33] M. C. Cross and P. C. Hohenberg, Pattern formation outside of equilibrium, Rev. Mod. Phys. **65**, 851 (1993).
[34] H. Nakao and A. S. Mikhailov, Turing patterns in network-organized activator-inhibitor systems, Nat. Phys. **6**, 544 (2010).
[35] J. Petit, B. Lauwens, D. Fanelli, and T. Carletti, Theory of Turing Patterns on Time Varying Networks, Phys. Rev. Lett. **119**, 148301 (2017).
[36] G. G. Rozenman, W. P. Schleich, L. Shemer, and A. Arie, Periodic Wave Trains in Nonlinear Media: Talbot Revivals, Akhmediev Breathers, and Asymmetry Breaking, Phys. Rev. Lett. **128**, 214101 (2022).
[37] W. Liu, J. Xiao, and J. Yang, Synchronization in coupled chaotic oscillators with a no-flux boundary condition, Phys. Rev. E **70**, 066211 (2004).